



## Preparation of poly(methyl methacrylate)-zinc oxide hybrid nanoparticles via miniemulsion polymerization

Tanapak Metanawin<sup>1</sup>, Maneerat Charoenchan<sup>2</sup> and Siripan Metanawin<sup>2,3\*</sup>

<sup>1</sup>Department of Materials and Production Technology Engineering, Faculty of Engineering, King Mongkut's University of Technology North Bangkok, Bangkok 10800, THAILAND

<sup>2</sup>Department of Textile Engineering, Faculty of Engineering, Rajamangala University of Technology Thanyaburi, Pathum Thani 12120, THAILAND

<sup>3</sup>Materials Design and Development (AMDD) Research Unit, Faculty of Engineering, Rajamangala University of Technology Thanyaburi, Pathum Thani 12120, THAILAND

\*Corresponding author: siripan.m@en.rmutt.ac.th

### ABSTRACT

The encapsulation of zinc oxide (ZnO) nanoparticles with poly(methyl methacrylate) in the presence of triethylene glycol dimethacrylate (TEGDMA) as a crosslinking agent was synthesized by the miniemulsion polymerization technique. The ZnO as a catalyze was varied from 1 wt% - 7 wt%. Several techniques were used to analyze the PMMA/TEGDMA/ZnO hybrid. The morphology and particle size distribution of the PMMA hybrid was observed using a field emission scanning electron microscope (FE-SEM). The diameter of the PMMA/TEGDMA/ZnO hybrid was in the range of 57 nm to 115 nm. The morphology of the PMMA/ZnO hybrids was sphere-shaped with a narrow particle size distribution and no agglomeration of the hybrids occurred. The encapsulation and crystalline structure of the PMMA ZnO hybrid were determined using a high-resolution transmission electron microscope (HR-TEM). The HR-TEM image demonstrated that the ZnO was encapsulated in the PMMA hybrid. In addition, the high magnification of the TEM image demonstrated the lattice spacing of ZnO and the diffraction mode image presented the crystalline structure of ZnO. Therefore, the photocatalytic properties of the PMMA/ZnO hybrid were examined via the degradation of methylene blue (MB) solution under dark and UV-A irradiation. It was found that the photocatalytic activities of the PMMA/ZnO hybrid increased when the ZnO content increased up to 7 wt%. The maximum MB degradation for PMMA/TEGDMA/ZnO 7 wt% and PMMA/ZnO 7 wt% were 80.1 % and 77.6 %, respectively. Thus, the photocatalytic efficiency of the PMMA/ZnO increased in the presence of TEGDMA as a crosslinking agent.

**Keywords:** Hybrid, Miniemulsion polymerization, Titanium dioxide, Poly(methyl methacrylate)

### INTRODUCTION

Hybrid materials have been widely studied because hybrid materials present the properties of both organic polymers and inorganic materials, with new properties [1, 2]. Hybrid materials comprise two or more materials on the molecular scale and nanoscale levels. The hybrid materials can design and synthesize novel materials in different techniques for sample use materials chemistry, inorganic chemistry, and polymer chemistry to make a new product such as electronic materials, efficient catalysts, magnetic materials, and optical material [1, 3, 4]. Various types of material combinations and synthesis strategies have been developed for the hybrid materials, using the sol-gel method, miniemulsion polymerization technique, or other solution processes [5-10].

Miniemulsion polymerization is a unique oil-in-water emulsion type with distinct advantages over conventional emulsion polymerization. Miniemulsion polymerization has several advantages: low reaction temperatures, high polymerization rate, high monomer conversion, and the ability to produce high molecular weight polymers [11-13]. Miniemulsion polymerization, consisting of tiny stable droplets within a size range of 50 nm to 500 nm, is usually prepared by shearing a mixture of monomer, surfactant, co-stabilizer, and initiator dispersed in an aqueous phase [9, 12, 14]. The most inorganic materials of photocatalysts and antibacterial are metal oxides such as zinc oxide (ZnO) and titanium dioxide (TiO<sub>2</sub>) [15, 16]. However, zinc oxide (ZnO) is one of the most popular photocatalysts and antibacterial agents because of its low cost and good stability. It has been widely used in a variety of

applications in the environment, including cosmetics, pigment, and air purification systems [17-20].

Several studies have focused on investigating the antibacterial and photocatalytic properties of ZnO. In previous studies, the PS/TEGDMA/TiO<sub>2</sub> hybrid demonstrated that the TEGDMA enhanced the photocatalytic properties and stability of the PS hybrid. Up to date, there are only a few studies on the encapsulation of ZnO via miniemulsion polymerization [21]. Furthermore, there is no research on PMMA/ZnO hybrid with TEGDMA via miniemulsion polymerization. Therefore, in this study, we synthesized the PMMA/ZnO hybrid via miniemulsion polymerization, and TEGDMA was added to the system as a crosslinking agent. The photocatalytic performance and the morphology of the hybrid were also studied.

## MATERIALS AND METHODS

### Materials

MMA monomer (99%, Sigma-Aldrich) was purified by passthrough basic aluminum oxide prior to use. Zinc oxide (ZnO, 99%, 10-30 nm, US Research Nanomaterials), aluminum oxide (basic Al<sub>2</sub>O<sub>3</sub>, Sigma-Aldrich), hexadecane (HD, 99%, Sigma-Aldrich), sodium dodecyl sulfate (SDS, 99%, Sigma-Aldrich), potassium persulfate (KPS, 99%, Sigma-Aldrich), triethylene glycol dimethacrylate (TEGDMA, 95%, Sigma-Aldrich), and methylene blue (MB, >95%, Ajax Finechem) were used as received. Deionized water (DI water) was purified by ELGA LabWater model Micra.

**Table1** The experimental details of the syntheses of PMMA/ZnO and PMMA/TEGDMA/ZnO.

Sample name	TEGDMA (% wt)	ZnO (% wt)
PMMA	-	-
PMMA/ZnO 1%	-	1
PMMA/ZnO 3%	-	3
PMMA/ZnO 7%	-	7
PMMA/TEGDMA	0.2	-
PMMA/TEGDMA/ZnO 1%	0.2	1
PMMA/TEGDMA/ZnO 3%	0.2	3
PMMA/TEGDMA/ZnO 7%	0.2	7

### Preparation of PMMA and PMMA/ZnO hybrid

In general, miniemulsion polymerization, 5.00 g of MMA, 0.20 g of hexadecane, and with/without 0.20 g of TEGDMA were mixed. 0.06 g of SDS was dissolved with 20.0 cm<sup>3</sup> of water in a flask. Then, the monomer mixture was added to the flask. It was stirred under nitrogen gas for 15 min. This flask was subjected

to ultrasound (130W and 60% amplitude) in an ice bath for 15 min to obtain miniemulsion. The reactor was heated to 70 °C and then, 0.083 g of KPS was added to the flask. After 4 h of reaction time, the miniemulsion was obtained by cooling it in an ice bath. The experimental details of the syntheses of PMMA/ZnO and PMMA/TEGDMA/ZnO using the miniemulsion technique are given in Table 1.

### Characterization

The structural analysis of the PMMA hybrid was measured using a PerkinElmer Frontier instrument (USA) spectrometer. The IR spectra were scanned between 4000-400 cm<sup>-1</sup>.

### Field Emission Scanning Electron Microscope (FE-SEM)

The PMMA hybrid morphology was discovered using a JSM-7600F (Jeol, Japan). The particle size distribution (average particle size) was measured from 20 samples using ImageJ software version 1.53e with Java 1.8.0\_172.

### High-resolution Transmission Electron Microscope (TEM)

The morphology and crystalline structure of the PMMA hybrid were performed on JEM-3100F (Jeol, Japan) operated at 300 kV.

### Photocatalytic activities

The photocatalytic activities were explored by detecting the degradation of MB under UV-A at 365 nm wavelength (TL-K 40W/10-R, Philips, The Netherlands). 1 mL of PMMA hybrids was placed in 10 ppm of MB. The light intensity was 6.0 mW/cm<sup>2</sup>. The samples were used directly without purification. The MB degradation was measured at a wavelength range of 660 nm using an UltraScan Pro Color dual-beam spectrophotometer with a 512-element diode array (HunterLab, USA).

## RESULTS AND DISCUSSION

### Effect of ZnO on morphology and structure of PMMA hybrid

The PMMA/ZnO and PMMA/TEGDMA/ZnO hybrids were synthesized by miniemulsion polymerization in the presence of TEGDMA as a crosslinking agent. The PMMA polymer was employed as a shell, whereas the ZnO was encapsulated in the core of the hybrid. Figure 1 shows the FE-SEM images and particle size distribution of the PMMA/TEGDMA/ZnO with various ZnO from 0, 1, 3, and 7 wt%. The result shows that the average diameter of PMMA/TEGDMA without ZnO was 57 nm, as seen in figures 1a and 1b while PMMA/TEGDMA/ZnO

1 wt% was 71 nm which the particle size increased by 24 %, as presented in Figure 1c and 1d. As seen in Figure 1e and 1f, moreover, the particle size of PMMA/TEGDMA/ZnO 3 wt% was 87 nm which increased by 52%. Therefore, the addition of ZnO 7 wt% to the PMMA hybrid increased the particle size to the maximum of 115 nm which increased 221%, as presented in Figure 1g and 1h. Figures 1b, 1d, 1f, and 1h presented the narrow size distribution of PMMA/TEGDMA/ZnO with various ZnO. From SEM images, the miniemulsion polymerization method exhibited an excellent particle size distribution without aggregation of ZnO nanoparticles. The addition of TEGDMA increased the stability of the PMMA hybrid resulting in no particle breakdown [22, 23]. It was noticed that the particle size of the PMMA hybrids increased with the amount of ZnO. This particle size increased due to a rise in the contents of ZnO in the PMMA hybrid  $\text{TiO}_2$  [24].

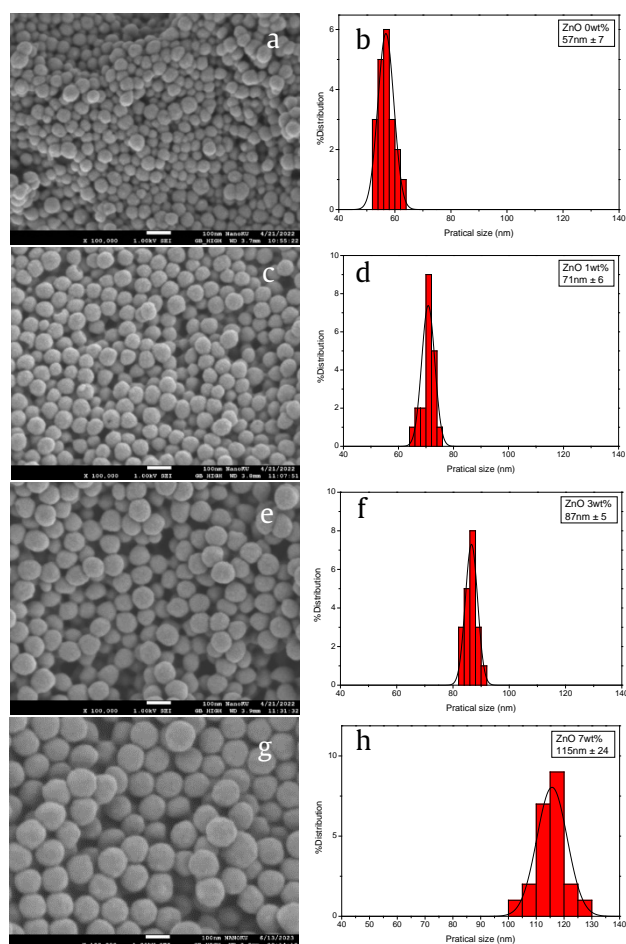
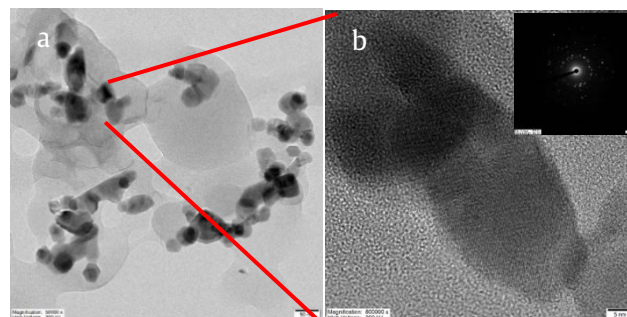


**Figure 1** FE-SEM image of PMMA/TEGDMA/ZnO 0, 1, 3, and 7 wt% at 100,000x magnifications. The scale bar was 100 nm.

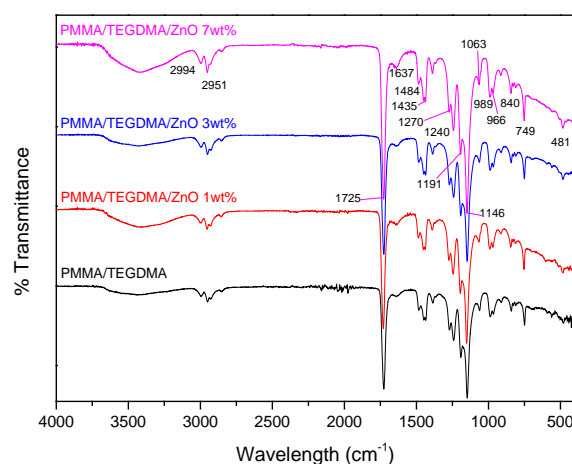
#### *Effect of ZnO on the structure of PMMA hybrid*

Figure 2 presented the HR-TEM image, lattice image, and diffraction pattern of the PMMA/TEGDMA/

ZnO 7wt%. Figure 2a demonstrates the encapsulation of ZnO in the PMMA/TEGDMA nanoparticles. Figure 2b shows the lattice of ZnO at a magnification of 500,000x. Inset demonstrated the diffraction mode, which was the crystalline structure of ZnO. It proved that the ZnO was successfully encapsulated in the PMMA hybrid.



**Figure 2** HR-TEM images of (a) PMMA/TEGDMA/ZnO 7 wt% at 100,000x magnifications and scale bar was 50 nm. (b) ZnO nanoparticle and the diffraction mode of ZnO nanoparticle at 500,000x magnifications and scale bar was 5 nm.



**Figure 3** The FT-IR spectra of the PMMA/TEGDMA/ZnO 0, 1, 3 and 7 wt%.

#### *Effect of ZnO on the functional of the hybrids*

The function group of the PMMA/TEGDMA/ZnO was discovered by FT-IR spectroscopy. Figure 3 shows the absorption bands at  $1063\text{ cm}^{-1}$  corresponding to  $-\text{C}-\text{O}-\text{C}-$ . The peaks observed at  $1146\text{ cm}^{-1}$  and  $1181\text{ cm}^{-1}$  were ascribed to ether carbon (C-O) bond stretching vibrations. The peaks observed at  $1725\text{ cm}^{-1}$  and  $1146\text{ cm}^{-1}$  were related to the stretching of the carbonyl group (C=O) and C=C groups, respectively [25]. The absorption bands appearing in the range of  $1488-1270\text{ cm}^{-1}$  are associated with  $\text{CH}_3$  and  $\text{CH}_2$  vibrational modes [25]. Furthermore, absorption bands at  $2951\text{ cm}^{-1}$  and  $2994\text{ cm}^{-1}$  corresponded to the asymmetric  $-\text{CH}_2$  stretching mode of PMMA [25]. The absorption band at  $1637\text{ cm}^{-1}$  is attributed to



the C=C stretching of the TEGDMA crosslinking agent [26, 27]. The vibration band at  $481\text{ cm}^{-1}$  was assigned to the stretching mode of the Zn-O bond [28]. The encapsulation of ZnO in the PMMA hybrid did not change the functional group of the PMMA due to the physical interaction of PMMA and ZnO. It is clearly seen that ZnO was presented in the PMMA hybrid miniemulsion.

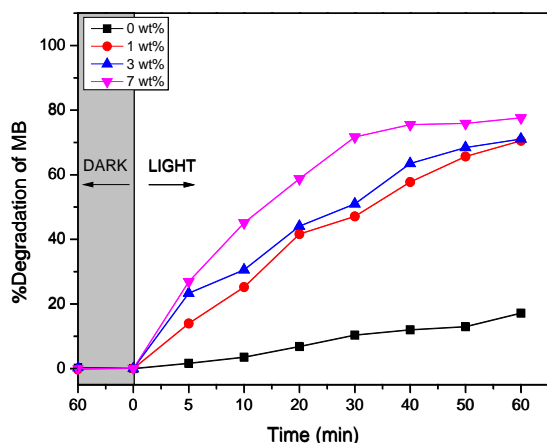


**Figure 4** The % degradation of the MB under dark and UV light conditions of PMMA/ZnO with ZnO 0, 1, 3, and 7 wt%.

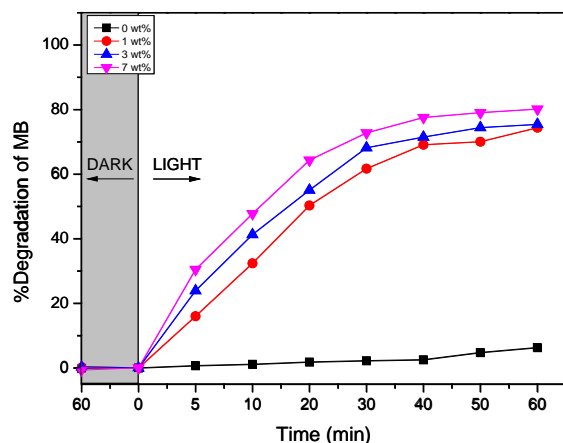


**Figure 5** The % degradation of the MB under dark and UV light conditions of PMMA/TEGDMA/ZnO with ZnO 0, 1, 3, and 7 wt%.

#### *Effect of ZnO on the photocatalytic of the hybrids*

The photocatalytic was investigated by monitoring the degradation of MB under UV illumination. The % degradation of PMMA/ZnO and PMMA/TEGDMA/ZnO with 0, 1, 3, and 7 wt% of ZnO contents were demonstrated in Figure 4 and Figure 5, respectively. The result shows that there was no MB absorption under dark conditions. Under UV illumination, the % degradation at 3 wt% (Figure 5) reached 55 % in 20 min, while the PMMA/

ZnO at 3% (Figure 4) spent 30 min to reach 51 % MB degradation. Therefore, the maximum MB degradation for PMMA/TEGDMA/ZnO 7 wt% and PMMA/ZnO 7 wt% were 80.1% and 77.6%, respectively. The TEGDMA increased the stability of the PMMA/ZnO hybrid by reducing particle breakage. This results in improved photocatalytic properties [22]. It is noticeable that the TEGDMA increased the photocatalytic capacity of the PMMA hybrid ZnO.

## CONCLUSION

The encapsulation of zinc oxide (ZnO) nanoparticles with poly(methyl methacrylate) by miniemulsion polymerization technique was successfully investigated. Triethylene glycol dimethacrylate (TEGDMA) was added to the system as a crosslinking agent in the presence of ZnO from 1 wt% - 7 wt%. The diameter and morphology of the PMMA/ZnO hybrid was in the range of 57 nm - 115 nm by using a field emission scanning electron microscope (FE-SEM). It was found that the diameter was slightly increased with the loading amount of ZnO from 1 wt% - 7 wt%. The HR-TEM images of the PMMA/TEGDMA/ZnO 0, 1, 3, and 7 wt% were studied to confirm the encapsulation of ZnO particles in the hybrid. It proved that the ZnO was successfully encapsulated in the PMMA hybrid. The functional group of the PMMA/ZnO hybrid was analyzed by Fourier Transform Infrared Spectroscopy (FTIR). It is clearly seen that the ZnO encapsulation PMMA/TEGDMA was successfully synthesized via the miniemulsion polymerization method. The photocatalytic properties of the PMMA/ZnO hybrid were also tested via the degradation of methylene blue (MB) solution under UV-A irradiation, and the photocatalytic activities increased when increasing ZnO contents up to 7 wt%.

## ACKNOWLEDGEMENT

This research was supported by The Science, Research and Innovation Promotion Funding (TSRI) (Grant no. FRB650070/0168). This research block grant was managed under Rajamangala University of Technology Thanyaburi (FRB65E0701C.1).

## REFERENCES

1. John Ł, Ejfler J. A brief review on selected applications of hybrid materials based on functionalized cage-like silsesquioxanes. *Polymers*. 2023;15(6):1452.
2. Young G, Tallia F, Clark JN, Chellappan M, Gavalda-Diaz O, Alcocer EJ, et al. Hybrid materials with continuous mechanical property gradients that can be 3D printed. *Mater Today Adv*. 2023;17:100344.

3. Zhang M, Gao G, Li C-Q, Liu F-Q. Titania-coated polystyrene hybrid microballs prepared with miniemulsion polymerization. *Langmuir*. 2004;20(4):1420-4.
4. Katagiri K. Chapter 5 - Organic-Inorganic Hybrid Nanoarchitecture at Mesoscale. In: Ariga K, Aono M, editors. *Supra-Materials Nanoarchitectonics*: William Andrew Publishing; 2017. p. 117-33.
5. Jahanzad F, Karatas E, Saha B, Brooks BW. Hybrid polymer particles by miniemulsion polymerisation. *Colloids Surf A: Physicochem Eng*. 2007;302(1-3):424-9.
6. Metanawin S, Metanawin T. Fabrication of hybrid polystyrene-titanium dioxide with enhanced dye degradation and antimicrobial properties: investigation of the effect of triethylene glycol dimethacrylate on photocatalytic activity. *Polym Int*. 2022;71(7):777-89.
7. Metanawin S, Sornsuwit N, Metanawin T. Miniemulsion polymerization technique enhancement: the photocatalysis of commercial rutile-TiO<sub>2</sub> hybrids with nano poly(methyl methacrylate). *Polym-Plast Technol Mater*. 2022; 61(1):56-68.
8. Metanawin T, Panutumrong P, Metanawin S. Synthesis of polyurethane/TiO<sub>2</sub> hybrid with high encapsulation efficiency using one-step miniemulsion polymerization for methylene blue degradation and its antibacterial applications. *ChemistrySelect*. 2023;8(11):e202204522.
9. Teo BM, Prescott SW, Ashokkumar M, Grieser F. Ultrasound initiated miniemulsion polymerization of methacrylate monomers. *Ultrason Sonochem*. 2008;15(1):89-94.
10. Livage J. Sol-gel synthesis of hybrid materials. *Bull Mater Sci*. 1999;22(3):201-5.
11. Landfester K. Synthesis of colloidal particles in miniemulsions. *Annu Rev Mater Res*. 2006;36(1): 231-79.
12. Rao JP, Geckeler KE. Polymer nanoparticles: Preparation techniques and size-control parameters. *Prog Polym Sci*. 2011;36(7):887-913.
13. Antonietti M, Landfester K. Polyreactions in miniemulsions. *Prog Polym Sci*. 2002;27(4):689-757.
14. Zhou J, Cui Y, Yao H, Ma J, Ren H. Nanocapsules containing binary phase change material obtained via miniemulsion polymerization with reactive emulsifier: Synthesis, characterization, and application in fabric finishing. *Polym Eng Sci*. 2019;59(s2):E42-51.
15. Khan MM, Adil SF, Al-Mayouf A. Metal oxides as photocatalysts. *J Saudi Chem Soc*. 2015;19(5): 462-4.
16. Disha KM. Metal oxide nanomaterials for photocatalytic degradation of antibiotics. *Mater Today: Proc*. 2023.
17. Yemmireddy VK, Hung YC. Using Photocatalyst metal oxides as antimicrobial surface coatings to ensure food safety-opportunities and challenges. *Compr Rev Food Sci F*. 2017;16(4):617-31.
18. Lu PJ, Huang SC, Chen YP, Chiueh LC, Shih DYC. Analysis of titanium dioxide and zinc oxide nanoparticles in cosmetics. *J Food Drug Anal*. 2015;23(3):587-94.
19. Agarwal H, Venkat Kumar S, Rajeshkumar S. A review on green synthesis of zinc oxide nanoparticles - An eco-friendly approach. *Resource-Efficient Technologies*. 2017;3(4):406-13.
20. Zhou XQ, Hayat Z, Zhang DD, Li MY, Hu S, Wu Q, et al. Zinc Oxide Nanoparticles: Synthesis, Characterization, Modification, and Applications in Food and Agriculture. *Processes*. 2023;11(4): 1193.
21. Fogaça LA, Feuser PE, Ricci-Júnior E, Hermes de Araújo PH, Sayer C, Costa C. ZnO and quercetin encapsulated nanoparticles for sun protection obtained by miniemulsion polymerization using alternative co-stabilizers. *Mater Res Express*. 2020;7(1):015096.
22. Al-Shannaq R, Farid M, Al-Muhtaseb S, Kurdi J. Emulsion stability and cross-linking of PMMA microcapsules containing phase change materials. *Sol Energ Mat Sol C*. 2015;132:311-8.
23. Liang K, Liu Q, Peng M. Monodisperse cross-linked polystyrene nanospheres by emulsifier-free miniemulsion polymerization. *e-Polym*. 2015;15(4):263-70.
24. Erdem B, Sudol ED, Dimonie VL, El-Aasser MS. Encapsulation of inorganic particles via miniemulsion polymerization. *Macromol Symp*. 2000;155(1): 181-98.
25. Singh S, Arora N, Paul K, Kumar R, Kumar R. FTIR and rheological studies of PMMA-based nano-dispersed gel polymer electrolytes incorporated with LiBF<sub>4</sub> and SiO<sub>2</sub>. *Ionics*. 2019;25(4):1495-503.
26. Ahangaran F, Navarchian AH. Towards the development of self-healing and antibacterial dental nanocomposites via incorporation of novel acrylic microcapsules. *Dent Mater J*. 2022;38(5): 858-73.

27. Hodášová L, Alemán C, del Valle LJ, Llanes L, Fargas G, Armelin E. 3D-Printed polymer-infiltrated ceramic network with biocompatible adhesive to potentiate dental implant applications. *Mater.* 2021;14(19):5513.
28. Nagaraju G, Udayabhanu, Shivaraj, Prashanth SA, Shastri M, Yathish KV, et al. Electrochemical heavy metal detection, photocatalytic, photoluminescence, biodiesel production and antibacterial activities of Ag-ZnO nanomaterial. *Mater Res Bull.* 2017;94:54-63.